Decomposition Based Stochastic Programming Approach for Polygeneration Energy Systems Design under Uncertainty

ARTICLE *in* INDUSTRIAL & ENGINEERING CHEMISTRY RESEARCH · FEBRUARY 2010

Impact Factor: 2.59 · DOI: 10.1021/ie901490g

Pei Liu
Tsinghua University

Zheng Li
Tsinghua University

Decomposition Based Stochastic Programming Approach for Polygeneration Energy Systems Design under Uncertainty

Pei Liu,[†] Efstratios N. Pistikopoulos,*[,†] and Zheng Li[‡]

Centre for Process Systems Engineering (CPSE), Department of Chemical Engineering, Imperial College London, London, SW7 2AZ, U.K., and Department of Thermal Engineering, Tsinghua University, Beijing, China, 100084

Polygeneration, a multi-input multioutput energy conversion process which typically involves the coproduction of electricity and liquid synthetic fuels, is a promising technology which offers real potential toward the reduction of excessive energy consumption and consequent greenhouse gas emissions. The optimal design of such a complex and nonlinear process system under inevitable and unpredictable future uncertainty poses great challenges in terms of both modeling and corresponding solution strategies. In this paper, we propose a stochastic programming framework for the optimal design under uncertainty of polygeneration energy systems. On the basis of a detailed mixed-integer nonlinear programming (MINLP) model, proposed in our previous work, a two-stage stochastic programming problem is formulated, which is then converted into a large-scale multiperiod MINLP problem by employing cubature based integration and sampling techniques. A decomposition algorithm is utilized for the efficient solution of the multiperiod problem, which involves iterations between a set of nonlinear subproblems of much smaller size and a master mixed-integer linear programming problem. A case study is then presented, where detailed computational results and comparisons between optimal designs obtained for both the stochastic and deterministic cases are shown.

Introduction

Polygeneration is an advanced multi-input multioutput energy conversion technology which exhibits much higher energy efficiency and lower greenhouse gas (GHG) emissions than conventional stand-alone power plants and chemical complexes.[1−6] A transition from the existing energy systems dominated by stand-alone processes to more advanced polygeneration energy systems could provide a meaningful way in order to reduce excessive energy consumption and GHG emissions. Moreover, a polygeneration plant typically coproduces electricity and chemical synthesis fuels, and these fuels can be used as substitutes for traditional oil based liquid fuels to release the current high pressure on oil production.

A typical schematic flowsheet of a polygeneration process is presented in Figure 1.[7] Its primary feedstock could be coal, petroleum coke, biomass, or a mixture of them. The feedstock is gasified in a gasifier with oxygen supplied from an air separation unit (ASU) to produce synthesis gas, or syngas, which comprises primarily carbon monoxide and hydrogen. After a series of cleanup procedures to remove ashes, residual carbon particles, and sulfur compounds, the fresh syngas is split between a power generation block and a chemical synthesis block to produce electricity and chemical liquid fuels simultaneously. Due to the high degree of integration between the power generation and chemical synthesis processes, the energy efficiency of a polygeneration plant is higher than the corresponding combination of a stand-alone power plant and chemical plant of the same capacity.

Besides improved energy efficiency, a polygeneration process also provides options for GHG emissions reduction at a reduced energy penalty. An optional water gas shift reactor and an optional carbon dioxide capture and sequestration (CCS) device can be added into a polygeneration process between the cleanup island and the syngas splitter. In the water gas shift reactor, carbon monoxide is converted to carbon dioxide and hydrogen, leading to high concentrations of carbon dioxide and hydrogen in the shifted syngas. Separating the carbon dioxide from the syngas requires less energy compared with the separation procedure in a stand-alone power plant, where the concentration of carbon dioxide in the fluegas is relatively low, resulting in an energy intensive separation procedure.

All these factors, while making polygeneration energy systems a potentially promising alternative technology, are also posing major challenges, especially toward the optimal design of such complex systems. In our previous works,[8−10] we have proposed a superstructure based mixed-integer optimization representation for the strategic planning and design of polygeneration energy systems, over a long-term horizon, under purely deterministic conditions. However, especially due to the long-term operational horizon, uncertainty is almost inevitable at the design phase of a polygeneration plant. Such uncertainty may be attributed to external factors,[11] such as market conditions (product demand, prices of feedstocks and products) and environmental constraints, and/or process related factors—such as fluctuation/variation in flow rates and stream composition, temperatures, efficiencies, and the like. The incorporation of such uncertainty considerations in the design of polygeneration energy systems poses further challenges and is the objective of this work.

In particular, we present a stochastic programming framework for the optimal design of polygeneration energy systems under uncertainty, which involves the following:

- a model representation of the uncertainty involved based on probability distribution functions
- a two-stage stochastic mixed-integer nonlinear programming (MINLP) model representation of the polygeneration energy systems design under uncertainty based on our previously proposed MINLP design model

* To whom correspondence should be addressed: E-mail: e.pistikopoulos@imperial.ac.uk.
[†] Imperial College London.
[‡] Tsinghua University.

10.1021/ie901490g
Published on Web 02/25/2010

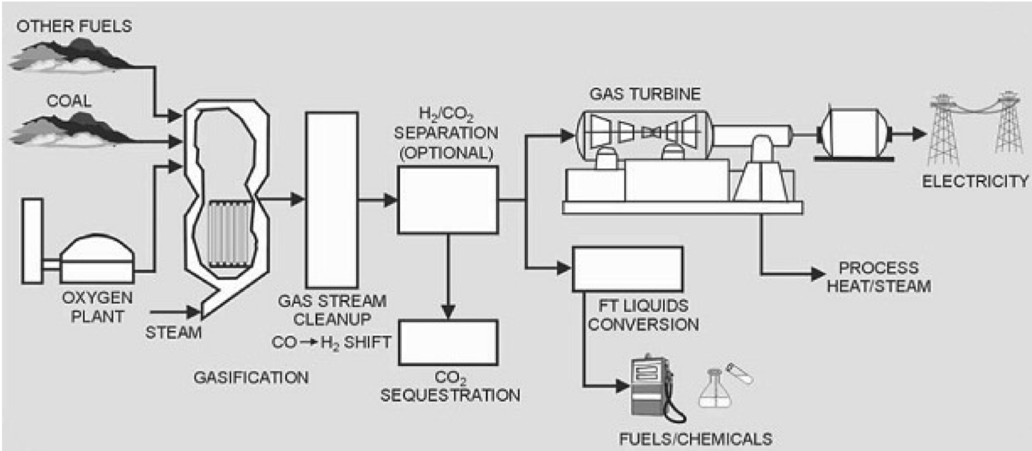

Figure 1. Schematic flowsheet of a polygeneration plant.

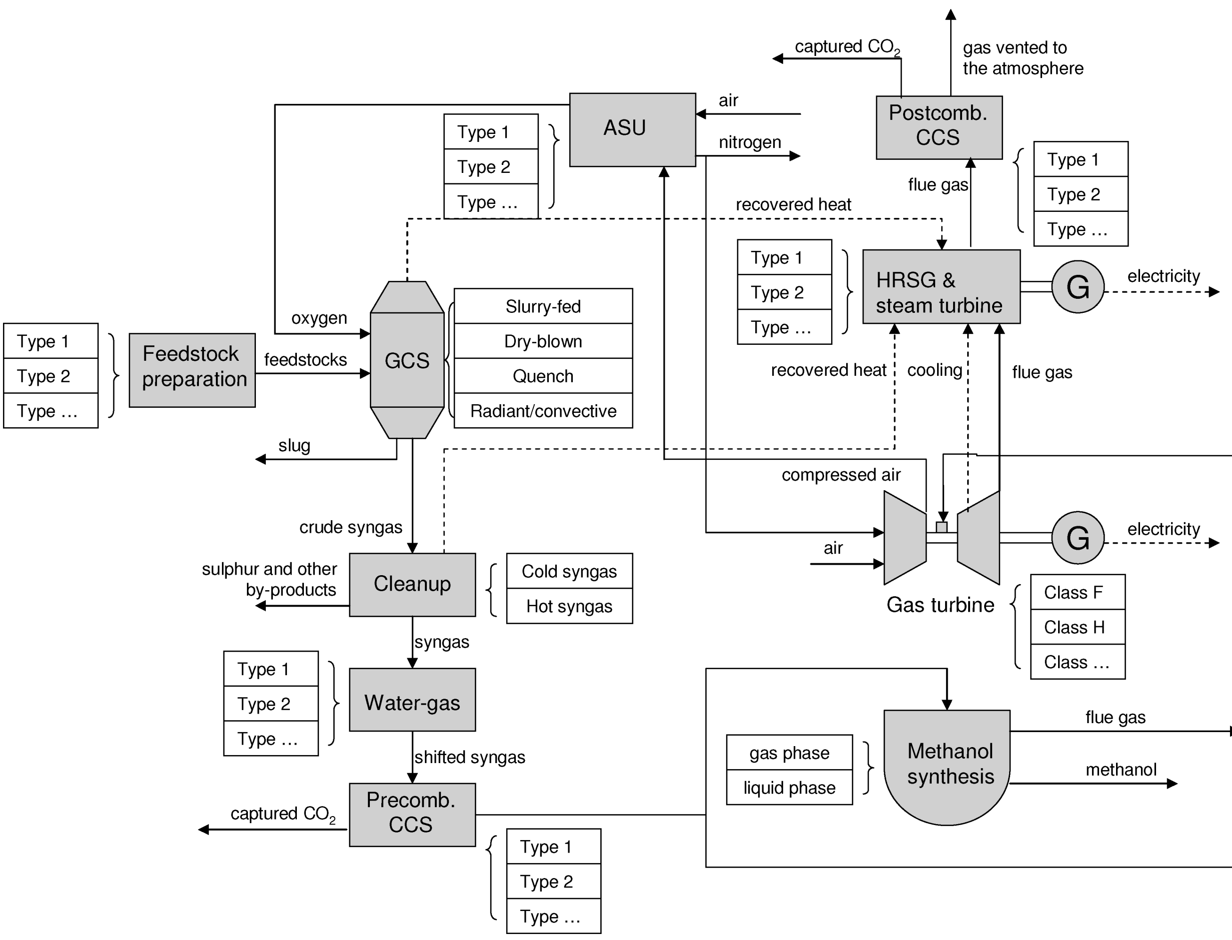

Figure 2. Superstructure representation of a polygeneration process.

- a numerical approximation of the stochastic terms by means of a cubature based integration and sampling technology, which allows for the reformulation of the two-stage stochastic problem into a large-scale multiperiod problem
- a decomposition algorithm[12,13] for the efficient solution and global optimum search of the underlying multiperiod MINLP design optimization problem.

The paper is organized as follows. The mathematical problem is introduced first, followed by a detailed description of the stochastic programming solution strategy. A detailed case study is finally presented, where comparisons between the deterministic and stochastic based designs are shown.

Polygeneration Energy Systems Design under Uncertainty: Mathematical Model

MINLP Design Optimization Model. In our previous work,[10] a superstructure based MINLP model is developed for the optimal process design of a typical polygeneration complex which coproduces methanol and electricity. Figure 2 shows the superstructure representation, where a polygeneration process is divided into ten key functional blocks, and all alternative technologies and types of equipment for a functional block are represented in terms of binary variables. The operation horizon of the polygeneration plant is discretized into n time intervals, $t \in \{t_1, t_2, ..., t_n\}$, where mass and energy balances are established between all these functional blocks. Moreover, a first-principle submodel for the chemical synthesis block is developed based on chemical kinetics and phase equilibrium and aggregated into the modeling framework. The mathematical formulation of this model is summarized in Appendix A. The proposed MINLP problem[14] is nonconvex, which can be solved to global optimality using GAMS/BARON.[15,16]

On the basis of the detailed MINLP model, we group the variables and equations/inequalities in the following way:

- binary design variables, denoted as vector $\mathbf{y}$, which represent the selection (or not) of technologies or types of equipment for each functional block, for instance, $y_{\mathrm{b\_gs}}$ for gasification technologies, $y_{\mathrm{b\_ms}}$ for methanol synthesis technologies, and the like
- continuous design variables, denoted as vector $\mathbf{d}$, which represent the capacities of the functional blocks, for instance, $\mathrm{cap}_{\mathrm{b\_gs}}$ for the coal processing capacity of the gasifier, $\mathrm{cap}_{\mathrm{b\_ms}}$ for the methanol synthesis capacity of the chemical synthesis block, and the like
- continuous operational variables, denoted as vector $\mathbf{x}_t$, which represent quantitative decisions to be made at each time interval t. All remaining variables in the model fall into this category, for instance, flow rates, stream compositions, and the like
- the objective function $\mathbf{f}$, which could be a scalar or a vector involving cost, profit, energy, and environmental behavior. In this work, net present value is used as the objective function, presented by eq a.52
- equality design constraints $\mathbf{h}^{\mathrm{dc}}$, which involves design variables $\mathbf{y}$ and $\mathbf{d}$ only, for instance, evaluation of initial investment costs. This category comprises eq a.46, and the like
- inequality design constraints $\mathbf{g}^{\mathrm{dc}}$, which involves design variables $\mathbf{y}$ and $\mathbf{d}$ only, for instance, logical relations between different functional blocks. This category comprises eq a.1, a.21, and the like
- equality operational constraints $\mathbf{h}^{\mathrm{oc}}$, which involves operational variables $\mathbf{x}_t$ and/or design variables $\mathbf{y}$ and $\mathbf{d}$. This category of constraints mainly come from the mass and energy balances calculation, comprising eqs a.2, a.5−a.19, a.23−a.38, a.40, a.42−a.43, a.45, a.47−a.52, and the like
- inequality operational constraints $\mathbf{g}^{\mathrm{oc}}$, which involves operational variables $\mathbf{x}_t$ and/or design variables $\mathbf{y}$ and $\mathbf{d}$. This category of constraints mainly come from the mass and energy balances calculation, comprising eqs a.3, a.4, a.20, a.22, a.39, a.41, a.44, and the like.

According to this classification, the MINLP problem presented in Appendix A can be recast in the following compact form:

$$
\begin{aligned}
\min_{\mathbf{y},\mathbf{d},\mathbf{x}_t}\quad & \mathbf{f}(\mathbf{y},\mathbf{d},\mathbf{x}_t) \\
\text{s.t.}\quad & \mathbf{h}^{\mathrm{dc}}(\mathbf{y},\mathbf{d}) = 0 \\
& \mathbf{g}^{\mathrm{dc}}(\mathbf{y},\mathbf{d}) \le 0 \\
& \mathbf{h}^{\mathrm{oc}}(\mathbf{y},\mathbf{d},\mathbf{x}_t) = 0 \\
& \mathbf{g}^{\mathrm{oc}}(\mathbf{y},\mathbf{d},\mathbf{x}_t) \le 0 \\
& \mathbf{d} \in \mathcal{R}^l, \mathbf{y} \in \{0,1\}^m, \mathbf{x}_t \in \mathcal{R}^n
\end{aligned}
\qquad \text{(d)}
$$

Uncertainty Considerations. In the above MINLP design optimization model d, all time-variant parameters are considered as piecewise constant functions over the operation horizon, which is discretized into several time intervals. However, due to the very nature of the long-term operation horizon, uncertainty is almost inevitable at the design stage, for example, due to external factors, such as market demands for products, prices of feedstocks and products, and the like. Here, we consider that all uncertain parameters can be presented as random variables following given probability distribution functions $p(x)$. The probability of an uncertain parameter θ lying in a given interval $[\theta^{\mathrm{L}}, \theta^{\mathrm{U}}]$ can thus be obtained by integration over this uncertain interval, as follows:

$$P(\theta^{\mathrm{L}} \le \theta \le \theta^{\mathrm{U}}) = \int_{\theta^{\mathrm{L}}}^{\theta^{\mathrm{U}}} p(\theta)\,\mathrm{d}\theta \qquad (1)$$

Two-Stage Stochastic Programming Formulation. By incorporating the uncertainty into the MINLP design problem, the following two-stage stochastic programming problem[17−19] results:

$$
\begin{aligned}
\min_{\mathbf{y},\mathbf{d}}\quad & f_{\mathrm{d}}(\mathbf{y},\mathbf{d}) + E_{\theta\in\Theta}[f_{\mathrm{s}}(\mathbf{y},\mathbf{d},\theta)] \\
\text{s.t.}\quad & \mathbf{h}^{\mathrm{dc}}(\mathbf{y},\mathbf{d}) = 0 \\
& \mathbf{g}^{\mathrm{dc}}(\mathbf{y},\mathbf{d}) \le 0 \\
& \mathbf{d} \in \mathcal{R}^l, \mathbf{y} \in \{0,1\}^m \\
\text{with:}\quad & \\
& f_{\mathrm{s}}(\mathbf{y},\mathbf{d},\boldsymbol{\theta}) = \min_{\mathbf{x}_t} f_{\mathrm{s}}(\mathbf{y},\mathbf{d},\mathbf{x}_t,\theta) \\
& \qquad \text{s.t.}\quad \mathbf{h}^{\mathrm{oc}}(\mathbf{y},\mathbf{d},\mathbf{x}_t,\theta) = 0 \\
& \qquad\qquad \mathbf{g}^{\mathrm{oc}}(\mathbf{y},\mathbf{d},\mathbf{x}_t,\theta) \le 0 \\
& \qquad\qquad \mathbf{x}_t \in \mathcal{R}^n \\
& \qquad\qquad \theta \in \Theta
\end{aligned}
\qquad \text{(p)}
$$

where the objective function is split into a deterministic term f_{d} representing decisions at the design stage and the expectation of a stochastic term f_{s} which depends on the realization of uncertain parameters θ at the operation stage. Discrete variables $\mathbf{y}$ and continuous variables $\mathbf{d}$ are "here-and-now" (design) variables which should be decided at the first-stage problem in p before the realizations of uncertain parameters θ occur, and $\mathbf{x}_t$ is a vector of "wait-and-see" (operational) variables which can be decided at time interval t of the second-stage problem in p where all uncertain parameters have been observed. In the second-stage problem, the recourse term based on a specific realization of uncertain parameters is optimized and corresponding corrective actions in terms of values of $\mathbf{x}_t$ are made.

A decomposition strategy for the solution of p is discussed next.

Decomposition Based Stochastic Programming Solution Strategy

The solution of problem p involves two major challenges: evaluation of the expectation of the stochastic term in the objective function of the first-stage problem and deriving an algorithm for the efficient solution of the two-stage problem. Here, a cubature based integration and sampling technique are employed to numerically approximate the expectation term, based on which the two-stage problem can be converted to a large-scale multiperiod optimization problem. Then, a decomposition strategy is introduced for its efficient solution.

Numerical Approximation of Stochastic Terms. The first-stage problem in problem p requires a proper evaluation of the expectation of the stochastic part of the objective function. Assuming the uncertain parameters θ follow a joint probability distribution $j(\theta)$, the expectation can be obtained via integration over the uncertain space Θ, as follows:

$$E_{\theta\in\Theta}[f_s(\mathbf{y},\mathbf{d},\theta)] = \int_{\Theta} f_s(\mathbf{y},\mathbf{d},\theta) j(\theta)\,d\theta \quad (2)$$

Cubature integration techniques are used to approximate the multidimensional integration in (2), using a one-dimensional quadrature over a certain number of sampling points for a given accuracy requirement.[20-22] On the basis of this, (2) can be rewritten as follows

$$\int_{\boldsymbol{\theta}} f_s(\theta) j(\theta)\,d\theta = \sum_{i}^{N_p} B_i f_s(\theta_i) \quad (3)$$

where B_i can be obtained by projecting the uncertainty space Θ to a normalized space U, as follows:

$$B_i = B_i^* |\det \mathrm{Jac}\ \theta(u_i)|, i = 1, 2, ..., N_p \quad (4)$$

Bernardo et al.[22] compared accuracy and computational performances of many integration formulas and provided mathematical expressions of N_p in terms of N_θ and expressions of B_i. These integration formulas comprise general product Gauss formula, n-cube cabatures, specialized product Gauss formula, and specialized cabatures of degrees of three, five, and seven, as shown in Appendix B.

Using eq 3 and 4, evaluation of an expectation term, as shown in eq 2, can be approximated via cubature formulas.

Multiperiod Formulation. By applying a suitable sampling and integration technique, as shown in the previous section, the two-stage stochastic programming problem p can be reformulated as a large-scale multiperiod problem, as follows:

$$\begin{aligned} \min_{\mathbf{y},\mathbf{d},\mathbf{x}_{t,i}} \quad & f_d(\mathbf{y},\mathbf{d}) + \sum_{i=1}^{N_p} B_i f_s(\mathbf{y},\mathbf{d},\mathbf{x}_{t,i},\theta_i) \\ \text{s.t.} \quad & \mathbf{h}^{dc}(\mathbf{y},\mathbf{d}) = 0 \\ & \mathbf{g}^{dc}(\mathbf{y},\mathbf{d}) \le 0 \\ & \left.\begin{aligned} &\mathbf{h}^{oc,i}(\mathbf{y},\mathbf{d},\mathbf{x}_{t,i},\theta_i) = 0 \\ &\mathbf{g}^{oc,i}(\mathbf{y},\mathbf{d},\mathbf{x}_{t,i},\theta_i) \le 0 \end{aligned}\right. \quad i = 1, ..., N_p \\ & \mathbf{d} \in \mathcal{R}^l, \mathbf{y} \in \{0,1\}^m, \mathbf{x}_t \in \mathcal{R}^n \end{aligned} \quad \text{(mp)}$$

In principle, this large-scale multiperiod problem can be solved directly. However, since the number of constraints involving operational variables is increased by a factor of N_p, the direct solution strategy could be computationally prohibitive. Next, a decomposition strategy is introduced for the efficient solution of this problem.

Decomposition Algorithm. Due to the formidable size of problem mp, it is desirable to take advantage of its block diagonal structure through a decomposition algorithm, thereby splitting it into several problems of smaller size. Here, the decomposition algorithm proposed by Ierapetritou and Pistikopoulos[12] and Ahmed et al.[13] is adopted. The algorithm splits the multiperiod problem into a master problem and a set of subproblems and solves them iteratively by continuously adding optimality and feasibility cuts based on dual information obtained from the solution of the subproblems. The steps of the algorithm are summarized below.

Step 0 (Initialization). Select an initial process design ($\mathbf{y}^0$, $\mathbf{d}^0$), and set the upper bound and lower bound of the original objective function to be UB = $+\infty$ and LB = $-\infty$, respectively.

Step 1. At iteration k, fix the process design obtained from last iteration $k - 1$ at ($\mathbf{y}^{k-1}$, $\mathbf{d}^{k-1}$), and solve the following nonlinear programming (NLP) subproblems at each cubature point:

$$\begin{aligned} \min_{\mathbf{x}_{t,i}} \quad & f_s(\mathbf{y}^{k-1},\mathbf{d}^{k-1},\mathbf{x}_{t,i},\theta_i) \\ \text{s.t.} \quad & \mathbf{h}^{oc}(\mathbf{y}^{k-1},\mathbf{d}^{k-1},\mathbf{x}_{t,i},\theta_i) = 0 \\ & \mathbf{g}^{oc}(\mathbf{y}^{k-1},\mathbf{d}^{k-1},\mathbf{x}_{t,i},\theta_i) \le 0 \\ & \mathbf{x}_t \in \mathcal{R}^n \end{aligned} \quad \text{(s)}$$

If the subproblem solved at cubature point i is infeasible, a feasible cut can be constructed using the extreme dual direction π_i^k obtained in solving the subproblem and added to the master problem in step 4. Here, however, feasibility cuts are omitted from the algorithm as our model is formulated in a way that for any feasible process design there are always feasible operation strategies available, i.e., for any given ($\mathbf{y}$, $\mathbf{d}$), problem s is always feasible.

Step 2. Evaluate the cubature integration of the original objective function. As it is obtained at a feasible solution of the original problem, it is a upper bound of the optimal solution, denoted as follows:

$$\mathrm{UB}^k = f_d(\mathbf{y}^{k-1},\mathbf{d}^{k-1}) + \sum_{i=1}^{N_p} B_i f_s(\mathbf{y}^{k-1},\mathbf{d}^{k-1},\mathbf{x}_{t,i}^k,\theta_i) \quad (5)$$

After obtaining the new upper bound, compare it with the existing upper bound UB and update correspondingly, as follows:

$$\mathrm{UB} = \min(\mathrm{UB}, \mathrm{UB}^k) \quad (6)$$

Step 3. Using the dual variables obtained from solving the subproblems, denoted as π_i^k, add an optimality cut to the master problem presented in step 4, as follows:

$$\mu \ge \sum_{i=1}^{N_p} B_i \cdot (\boldsymbol{\pi}_i^k \cdot \tau_i^T(\mathbf{y},\mathbf{d})) \quad (7)$$

where $\tau_i^T(\mathbf{y}, \mathbf{d})$ is a vector of functions of $\mathbf{y}$ and $\mathbf{d}$, obtained by separating terms involving $\mathbf{y}$ and $\mathbf{d}$ from the remaining terms.

Step 4. Obtain a lower bound by solving the following master mixed-integer linear programming (MILP) problem:

$$\begin{aligned} \min_{\mathbf{y},\mathbf{d}} \quad & f_d(\mathbf{y},\mathbf{d}) + \mu \\ \text{s.t.} \quad & \mathbf{h}^{dc}(\mathbf{y},\mathbf{d}) = 0 \\ & \mathbf{g}^{dc}(\mathbf{y},\mathbf{d}) \le 0 \\ & \mu \ge \sum_{i=1}^{N_p} B_i \cdot (\pi_i^l \cdot \tau_i^T(\mathbf{y},\mathbf{d})), l = 1, ..., k \\ & \mathbf{d} \in \mathcal{R}^l, \mathbf{y} \in \{0,1\}^m \end{aligned} \quad \text{(m)}$$

The solution of problem m also provides a new design {$\mathbf{y}$, $\mathbf{d}$}.

Step 5. Compare the gap between the lower and upper bounds with a convergence criterion ε. If UB $-$ LB $\le \varepsilon$, stop—the optimal solution is obtained at the current UB; else update {$\mathbf{y}$, $\mathbf{d}$} and go back to step 1. The optimality cuts added in step 3 keep on updating the lower bound obtained in step 4 until the convergence criterion set here is satisfied, thus convergence of the algorithm is guaranteed.[12,13]

Case Study

To further illustrate the proposed framework of optimal polygeneration process design under uncertainty, the entire

Table 1. Mean Values and Variances of Uncertain Parameters

uncertain parameter	mean value	variance
coal price ($/tonne)	65	6.5
electricity price ($/(kW h))	0.06	0.006
methanol price ($/tonne)	343	34.3
electricity demand (MW)	400	40
methanol demand (tonne/day)	500	50

framework has been applied in a case study for a polygeneration plant that coproduces methanol and electricity. All settings of this case study are kept the same as those of the case study presented in our previous work conducted using deterministic methods, so that the optimal designs for the same polygeneration plant obtained via both deterministic and stochastic means can be compared. Assumptions, data, and other details of the case study can be obtained from refs 10 and 14.

Five parameters, with significant impact on the process design, are selected as uncertain parameters, namely the coal price, electricity price, methanol price, electricity demand, and methanol demand. All five parameters are assumed to follow a normal distribution $\theta \sim N(\mu, \sigma^2)$. Mean values and variances of these five uncertain parameters are given in Table 1. Here, variances of these parameters are assumed to be 10% of their mean values, i.e., there is a probability of approximately 68.2% $(1 - \sigma)$ that the fluctuation of an uncertain parameter falls within $\pm$10% of its normal value.

As all uncertain parameters follow a normal distribution, the distribution of vector θ in the uncertain space also follows the normal distribution of $\theta \sim N(\mu, \Sigma)$. For specialized cubature $S_{5,1}$, the mapping between θ and u is given as follows:

$$\theta = \theta(u) = \mu + \sqrt{2}I\Sigma^{1/2}u \tag{8}$$

Assuming that there are no correlations between the uncertain parameters, the matrix Σ becomes a diagonal matrix where the diagonal elements are σ^2. Then a one-to-one mapping between an uncertain parameter and a sampling point can be established as follows:

$$\theta_i = \mu_i + \sqrt{2}\sigma_i u_i \tag{9}$$

Using eq b.2−b.7, 8, and 9, values of 42 sampling points u_i, coefficients B_i, and corresponding θ_i are obtained, as summarized in Table 2.

A multiperiod problem is then formulated, involving 9 binary design variables, 53 continuous design variables, 34 020 continuous operational variables, 4975 inequality constraints, and 30 826 equality constraints. Using BARON/GAMS to solve this problem, a direct solution cannot be obtained within 24 h on a 2000 MHz CPU with 16 GB memory.

Then, the decomposition algorithm is applied. The master problem involves 9 binary design variables, 53 continuous design variables, 19 inequality constraints, and 40 equality constraints. Each NLP subproblem involves 810 continuous operational variables, 118 inequality constraints, and 733 equality constraints. The overall algorithm takes 19 iterations and 283 min of CPU time to obtain the optimal solution. Note that while the overall large-scale problem can be solved to global optimality, the decomposition-based strategy is basically a global optimum search without theoretical guarantee for a global optimal solution.[23,24] Values of lower and upper bounds are presented in Figure 3 (note that the optimization direction in the case study is maximization, thus the lower and upper bounds are opposite to those defined in the decomposition algorithm).

Note that the obtained optimal design under uncertainty involves the same functional blocks as those selected in the deterministic optimal design, but with increased capacity, increased investment costs, and decreased net present value, as shown in Table 3.

Note also that an advantage of the process design under uncertainty is the increased envelope of feasible operation under different conditions. A one-to-one mapping from the normalized feasible operation region to the operation region in the uncertain parameter space can be established. On the basis of this, the exact size of the feasible operation space, denoted as the flexibility index F, could be obtained from eqs b.4 and 8, as follows:

$$F = \left|\frac{\theta_i}{\mu_i}\right| = 1 + \frac{\sqrt{2}\sigma_i u_i}{\mu_i} = 1 + \sqrt{2}\sqrt{\frac{N_\theta + 2}{2(N_\theta - 2)}}\frac{\sigma_i}{\mu_i} = 1 + \sqrt{\frac{N_\theta + 2}{N_\theta - 2}}\frac{\sigma_i}{\mu_i} \tag{10}$$

Here, N_θ is the number of uncertain parameters, five in this case study. Variances σ_i are assumed to be 10% of their mean values μ_i, thus the value of the term σ_i/μ_i is 0.1 here. Substituting the terms in eq 10 with their values, the flexibility index F is obtained, with a value of 1.153 in this case study.

The value of the flexibility index F indicates that feasible operation is guaranteed over an uncertain space where the fluctuation of each uncertain parameter is within $\pm$15.3% of its normal value. In terms of robustness, this design is superior to the one obtained using the deterministic modeling framework, where feasible operation is only guaranteed at the normal design point. The increased range of feasibility is obtained at a price of a reduced expected net present value, 25.7% lower than the deterministic design. This decrease is mainly due to increased design capacity of all major functional blocks, which enhances the capability of a polygeneration plant in dealing with changing market demands. As a result, the entire investment costs of the plant increase by 11.5%, accounting for 93.8% of the decrease in net present value.

Compared with the deterministic optimal design, the optimal design under uncertainty results in a more cautious strategy to enhance its flexibility, which leads to the reduction in plant profitability. However, this drop in profitability could be compensated in scenarios where a penalty is imposed for infeasible operation, for instance, for not meeting the market demand. If a 50% penalty is imposed on the electricity production, i.e., a plant needs to pay 50% of the worth of

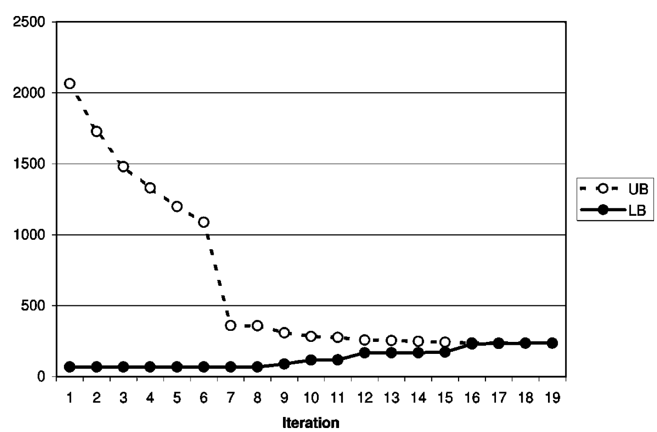

Figure 3. Lower and upper bounds obtained in the decomposition solution procedure.

Table 2. Values of Sampling Points, Coefficients, and Corresponding Uncertain Parameters

no.	sampling points					coefficient	uncertain parameters					
1	1.32	0	0	0	0	1.43	77	0.06	343	400	500
2	0	1.32	0	0	0	1.43	65	0.071	343	400	500
3	0	0	1.32	0	0	1.43	65	0.06	407	400	500
4	0	0	0	1.32	0	1.43	65	0.06	343	475	500
5	0	0	0	0	1.32	1.43	65	0.06	343	400	594
6	−1.32	0	0	0	0	1.43	53	0.06	343	400	500
7	0	−1.32	0	0	0	1.43	65	0.049	343	400	500
8	0	0	−1.32	0	0	1.43	65	0.06	279	400	500
9	0	0	0	−1.32	0	1.43	65	0.06	343	325	500
10	0	0	0	0	−1.32	1.43	65	0.06	343	400	406
11	1.08	1.08	1.08	1.08	1.08	0.1	75	0.069	395	461	576
12	−1.08	1.08	1.08	1.08	1.08	0.1	55	0.069	395	461	576
13	1.08	−1.08	1.08	1.08	1.08	0.1	75	0.051	395	461	576
14	−1.08	−1.08	1.08	1.08	1.08	0.1	55	0.051	395	461	576
15	1.08	1.08	−1.08	1.08	1.08	0.1	75	0.069	291	461	576
16	−1.08	1.08	−1.08	1.08	1.08	0.1	55	0.069	291	461	576
17	1.08	−1.08	−1.08	1.08	1.08	0.1	75	0.051	291	461	576
18	0	0	0	−1.08	0	0.1	65	0.06	343	339	500
19	1.08	1.08	1.08	−1.08	1.08	0.1	75	0.069	395	339	576
20	−1.08	1.08	1.08	−1.08	1.08	0.1	55	0.069	395	339	576
21	1.08	−1.08	1.08	−1.08	1.08	0.1	75	0.051	395	339	576
22	−1.08	−1.08	1.08	−1.08	1.08	0.1	55	0.051	395	339	576
23	1.08	1.08	−1.08	−1.08	1.08	0.1	75	0.069	291	339	576
24	−1.08	1.08	−1.08	−1.08	1.08	0.1	55	0.069	291	339	576
25	1.08	−1.08	−1.08	−1.08	1.08	0.1	75	0.051	291	339	576
26	−1.08	−1.08	−1.08	−1.08	1.08	0.1	55	0.051	291	339	576
27	1.08	1.08	1.08	1.08	−1.08	0.1	75	0.069	395	461	424
28	−1.08	1.08	1.08	1.08	−1.08	0.1	55	0.069	395	461	424
29	1.08	−1.08	1.08	1.08	−1.08	0.1	75	0.051	395	461	424
30	−1.08	−1.08	1.08	1.08	−1.08	0.1	55	0.051	395	461	424
31	1.08	1.08	−1.08	1.08	−1.08	0.1	75	0.069	291	461	424
32	−1.08	1.08	−1.08	1.08	−1.08	0.1	55	0.069	291	461	424
33	1.08	−1.08	−1.08	1.08	−1.08	0.1	75	0.051	291	461	424
34	0	0	0	−1.08	−1.08	0.1	65	0.06	343	339	424
35	1.08	1.08	1.08	−1.08	−1.08	0.1	75	0.069	395	339	424
36	−1.08	1.08	1.08	−1.08	−1.08	0.1	55	0.069	395	339	424
37	1.08	−1.08	1.08	−1.08	−1.08	0.1	75	0.051	395	339	424
38	−1.08	−1.08	1.08	−1.08	−1.08	0.1	55	0.051	395	339	424
39	1.08	1.08	−1.08	−1.08	−1.08	0.1	75	0.069	291	339	424
40	−1.08	1.08	−1.08	−1.08	−1.08	0.1	55	0.069	291	339	424
41	1.08	−1.08	−1.08	−1.08	−1.08	0.1	75	0.051	291	339	424
42	−1.08	−1.08	−1.08	−1.08	−1.08	0.1	55	0.051	291	339	424

electricity which it fails to deliver to the market, the net present value of the deterministic design would drop by 16.1% in a scenario where the market demand for electricity increases by 10%. In this case, the economic behavior of both the deterministic design and the design under uncertainty is approximately at the same level, hence a decision maker would tend to choose a more cautious design to reduce potential operation risks.

Table 3. Results Comparison between Deterministic and Stochastic Programming Problems

	deterministic	stochastic	difference
objective function			
NPV (million \$)	317.1	235.7	−25.7%
key design variables			
capacity of ASU (kg/s oxygen)	33.5	38.8	+15.8%
capacity of the gasifier (kg/s coal)	36.2	42.0	+15.8%
capacity of the syngas cleanup unit (kg/s syngas)	67.0	77.6	+15.8%
capacity of the methanol synthesis unit (kg/s methanol)	5.79	6.87	+18.7%
capacity of the gas turbine (MW)	273.0	324.9	+19.0%
capacity of the HRSG and steam turbines block (MW)	182.4	214.7	+17.7%
investment costs (million \$)	662.8	739.2	+11.5%

Conclusions

Optimization under uncertainty provides means to improve the robustness of a polygeneration energy systems design under future uncertainty. By reformulating a deterministic design problem into a two-stage stochastic programming problem, the potential impacts of uncertain parameters are accounted for while the underlying mathematical structure of the deterministic problem is retained. Making use of the block diagonal structure of the resulting multiperiod problem, an efficient decomposition strategy can be employed, where subproblems of much smaller size are solved iteratively. The size of this problem can be further reduced if specialized cubature integration methods are used to generate sampling points with computational advantages. A process design obtained via optimization under uncertainty provides a much larger envelope of feasible operation than a corresponding deterministic design, while properly balancing economic profitability and risk.

Acknowledgment

The authors gratefully acknowledge the financial support from BP. P.L. thanks the Kwoks' Foundation for providing an additional scholarship.

Appendix A: Mathematical Formulation of the MINLP Design Optimization Model

A detailed MINLP model for polygeneration process design,[10] based on the superstructure representation shown in Figure 2, is presented here.

First, the operating horizon is discretized into n_t time intervals, denoted as

$$t = \{t_1, t_2, ... t_{n_t}\}$$

In each time interval, mass and energy balances are established for all functional blocks. Aggregated models are considered to establish input−output relationships based on a reference variable, for each functional block. A more detailed mechanistic model is considered for the methanol synthesis block to appropriately capture the chemical kinetics and phase equilibrium relationships.

For conciseness, submodels of two typical functional blocks, namely the gasifier block and the methanol synthesis block, are presented here, followed by evaluations of production rates and the objective function. Nomenclature for all variables, parameters, and subscripts are listed in the Notation section.

Gasifier Block. The gasifier block includes several technical options. The selection (or not) of each technology is represented by a binary variable y_{ag}, while the following logical constraint:

$$\sum_{\mathrm{ag}} y_{\mathrm{b\_gs}}(\mathrm{ag}) \le 1 \tag{a.1}$$

enforces that only one technology can be selected (at most).

Mass balance constraints on the total flow rate of coal are given by

$$\mathrm{ma}_{\mathrm{b\_cp,drc},i}(t) = \sum_{\mathrm{ag}} \mathrm{ma}_{\mathrm{b\_cp,t\_gs,drc},i}(\mathrm{ag}, t) \tag{a.2}$$

with upper bound/lower bound constraints as follows

$$0 \le \mathrm{ma}_{\mathrm{b\_cp,t\_gs,drc,i}}(\mathrm{ag}, t) \le y_{\mathrm{b\_gs}}(\mathrm{ag}) \cdot \mathrm{UB} \tag{a.3}$$

The coal flow rate should never exceed the processing capacity of a gasifier, as follows:

$$\mathrm{ma}_{\mathrm{b\_cp,t\_gs,drc,i}}(\mathrm{ag}, t) \le \mathrm{cap}_{\mathrm{b\_gs}}(\mathrm{ag}) \tag{a.4}$$

Inputs to this block comprise coal slurry or oxygen-blown pulverized coal, oxygen from the ASU block, steam or water injection from the steam turbine to the gasification chamber, and making-up water to the syngas scrubber. Outputs are crude syngas, slag slurry, and blown-down water. Each gasifier requires a specific amount of oxygen to gasify the inlet coal, using the flow rate of inlet coal as the reference variable:

$$\mathrm{ma}_{\mathrm{b\_gs,t\_gs,oxy,i}}(\mathrm{ag}, t) = \alpha_{\mathrm{oxy/drc}}(\mathrm{ag}) \cdot \mathrm{ma}_{\mathrm{b\_cp,t\_gs,drc,i}}(\mathrm{ag}, t) \tag{a.5}$$

Oxygen streams split to all gasifiers coming from the ASU block:

$$\sum_{\mathrm{ag}} \mathrm{ma}_{\mathrm{b\_gs,t\_gs,oxy,i}}(\mathrm{ag}, t) = \mathrm{ma}_{\mathrm{b\_as,oxy,o}}(t) \tag{a.6}$$

Flowrates of steam/water injection, making-up water, slag slurry, and blown-down water are proportional to the reference variable, given by

$$\mathrm{ma}_{\mathrm{b\_gs,t\_gs,swi,i}}(\mathrm{ag}, t) = \alpha_{\mathrm{swi/drc}}(\mathrm{ag}) \cdot \mathrm{ma}_{\mathrm{b\_cp,t\_gs,drc,i}}(\mathrm{ag}, t) \tag{a.7}$$

$$ma_{\mathrm{b\_gs,t\_gs,mkw,i}}(\mathrm{ag}, t) = \alpha_{\mathrm{mkw/drc}}(\mathrm{ag}) \cdot \mathrm{ma}_{\mathrm{b\_cp,t\_gs,drc,i}}(\mathrm{ag}, t) \tag{a.8}$$

$$\mathrm{ma}_{\mathrm{b\_gs,t\_gs,bld,i}}(\mathrm{ag}, t) = \alpha_{\mathrm{bld/drc}}(\mathrm{ag}) \cdot \mathrm{ma}_{\mathrm{b\_cp,t\_gs,drc,i}}(\mathrm{ag}, t) \tag{a.9}$$

$$\mathrm{ma}_{\mathrm{b\_gs,t\_gs,ssl},o}(\mathrm{ag}, t) = \alpha_{\mathrm{ssl/drc}}(\mathrm{ag}) \cdot \mathrm{ma}_{\mathrm{b\_cp,t\_gs,drc,i}}(\mathrm{ag}, t) \tag{a.10}$$

Mass balance between the crude syngas and all other streams is established as follows:

$$\begin{aligned} &\mathrm{ma}_{\mathrm{b\_gs,t\_gs,csg,o}}(\mathrm{ag}, t) + ma_{\mathrm{b\_gs,t\_gs,ssl,o}}(\mathrm{ag}, t) = \\ &\quad \mathrm{ma}_{\mathrm{b\_cp,t\_gs,drc,i}}(\mathrm{ag}, t) + \mathrm{ma}_{b\mathrm{\_cp,t\_gs,csl,o}}(\mathrm{ag}, t) + \\ &\quad \mathrm{ma}_{b\mathrm{\_cp,t\_gs,oxy,o}}(\mathrm{ag}, t) + \mathrm{ma}_{\mathrm{b\_gs,t\_gs,oxy,i}}(\mathrm{ag}, t) + \\ &\quad \mathrm{ma}_{\mathrm{b\_gs,t\_gs,mkw,i}}(\mathrm{ag}, t) + \mathrm{ma}_{\mathrm{b\_gs,t\_gs,bld,i}}(\mathrm{ag}, t) \end{aligned} \tag{a.11}$$

Primary components in the crude syngas are H_2, CO, CO_2, H_2O, N_2, and H_2S, involving five elements: C, H, O, N, S. From mass balances for all the five elements, together with a mass relationship between H_2 and CO in the crude syngas, mole flow rates of each component in the crude syngas are determined through eq a.12−a.18:

$$\begin{aligned} \frac{\mathrm{ma}_{\mathrm{b\_cp,t\_gs,drc,i}}(\mathrm{ag}, t) \cdot \mathrm{UA}(C)}{\mathrm{MW}(C)} &= m_{\mathrm{b\_gs,t\_gs,c\bar{s}}g\mathrm{,o}}(\mathrm{ag}, \mathrm{CO}, t) + \\ &\quad m_{\mathrm{b\_gs,t\_gs,c\bar{s}g,o}}(\mathrm{ag}, \mathrm{CO_2}, t) \end{aligned} \tag{a.12}$$

$$\begin{aligned} &\frac{\mathrm{ma}_{\mathrm{b\_cp,t\_gs,drc,i}}(\mathrm{ag}, t) \cdot \mathrm{UA(H)}}{\mathrm{MW(H)}} + \\ &2\frac{\mathrm{ma}_{\mathrm{b\_cp,t\_gs,csl,o}}(\mathrm{ag}, t) + \mathrm{ma}_{\mathrm{b\_gs,t\_gs,mkw,i(ag,}t)} + \mathrm{ma}_{\mathrm{b\_gs,t\_gs,bld,i(ag,}t)}}{\mathrm{MW(H_2O)}} = \\ &2m_{\mathrm{b\_gs,t\_gs,c\bar{s}g,o}}(\mathrm{ag}, \mathrm{H_2}, t) + 2m_{\mathrm{b\_gs,t\_gs,c\bar{s}g,o}}(\mathrm{ag}, \mathrm{H_2O}, t) + \\ &2m_{\mathrm{b\_gs,t\_gs,c\bar{s}g,o}}(\mathrm{ag}, \mathrm{H_2S}, t) + \\ &2\frac{\mathrm{ma}_{\mathrm{b\_gs,t\_gs,ssl,o}}(\mathrm{ag}, t) - \mathrm{ma}_{\mathrm{b\_cp,t\_gs,drc,i}}(\mathrm{ag}, t) \cdot \mathrm{UA(ash)}}{\mathrm{MW(H_2O)}} \end{aligned} \tag{a.13}$$

$$\begin{aligned} &\frac{\mathrm{ma}_{\mathrm{b\_cp,t\_gs,drc,i}}(\mathrm{ag}, t) \cdot \mathrm{UA(O)}}{\mathrm{MW(O)}} + 2(m_{\mathrm{b\_gs,t\_gs,oxy,i}}(\mathrm{ag}, t) + \\ &m_{b\mathrm{\_cp,t\_gs,oxy,o}}(\mathrm{ag}, t)) \cdot X_{\mathrm{aox}}(\mathrm{O_2}) + \frac{\mathrm{ma}_{\mathrm{b\_gs,t\_gs,bld,i}}(\mathrm{ag}, t)}{\mathrm{MW(H_2O)}} = \\ &m_{\mathrm{b\_gs,t\_gs,c\bar{s}g,o}}(\mathrm{ag}, \mathrm{H_2O}, t) + m_{\mathrm{b\_gs,t\_gs,c\bar{s}g},o}(\mathrm{ag}, \mathrm{CO}, t) + \\ &2m_{\mathrm{b\_gs,t\_gs,c\bar{s}g,o}}(\mathrm{ag}, \mathrm{CO_2}, t) + \\ &\frac{\mathrm{ma}_{\mathrm{b\_gs,t\_gs,ssl,o}}(\mathrm{ag}, t) - \mathrm{ma}_{\mathrm{b\_cp,t\_gs,drc,i}}(\mathrm{ag}, t) \cdot \mathrm{UA(ash)}}{\mathrm{MW(H_2O)}} \end{aligned} \tag{a.14}$$

$$\begin{aligned} &\frac{\mathrm{ma}_{\mathrm{b\_cp,t\_gs,drc,i}}(\mathrm{ag}, t) \cdot \mathrm{UA(N)}}{\mathrm{MW(N)}} + 2(m_{\mathrm{b\_gs,t\_gs,oxy,i}}(\mathrm{ag}, t) + \\ &m_{\mathrm{b\_cp,t\_gs,oxy,o}}(\mathrm{ag}, t)) \cdot X_{\mathrm{aox}}(\mathrm{N_2}) = 2m_{\mathrm{b\_gs,t\_gs,c\bar{s}g,o}}(\mathrm{ag}, \mathrm{N_2}, t) \end{aligned} \tag{a.15}$$

$$\frac{\mathrm{ma}_{\mathrm{b\_cp,t\_gs,drc,i}}(\mathrm{ag}, t)\cdot \mathrm{UA(S)}}{\mathrm{MW(S)}} = m_{\mathrm{b\_gs,t\_gs,c\vec{s}g,o}}(\mathrm{ag}, \mathrm{H_2S}, t) \tag{a.16}$$

$$m_{\mathrm{b\_gs,t\_gs,c\vec{s}g,o}}(\mathrm{ag}, \mathrm{H_2}, t) = \alpha_{\mathrm{hyd/cm}}\cdot m_{\mathrm{b\_gs,t\_gs,c\vec{s}g,o}}(\mathrm{ag}, \mathrm{CO}, t) \tag{a.17}$$

Finally, crude syngas exiting all gasifiers is mixed up for further cleaning in downstream cleanup units.

$$m_{\mathrm{b\_gs,c\vec{s}g,o}}(\mathrm{is}, t) = \sum_{\mathrm{ag}} m_{\mathrm{b\_gs,t\_gs,c\vec{s}g,is}}(\mathrm{ag}, \mathrm{is}, t) \tag{a.18}$$

Methanol Synthesis. Two mechanistic models are considered for the gas phase and liquid phase methanol synthesis based on chemical kinetics and phase equilibrium,[25] to handle different mole compositions of the inlet sweet syngas resulted from different gasification technologies used upstream.

First, the sweet syngas is split between gas and liquid phase methanol synthesis. Only one technology can be selected.

$$m_{\mathrm{b\_c1,s\vec{s}g,o}}(\mathrm{is}, t) = \sum_{\mathrm{am}} m_{\mathrm{b\_ms,t\_ms,s\vec{s}g,i}}(\mathrm{am}, \mathrm{is}, t) \tag{a.19}$$

$$0 \le m_{\mathrm{b\_ms,t\_ms,s\vec{s}g,i}}(\mathrm{am}, \mathrm{is}, t) \le y_{\mathrm{b\_ms}}(\mathrm{am})\cdot \mathrm{UB} \tag{a.20}$$

$$\sum_{\mathrm{am}} y_{\mathrm{b\_ms}}(\mathrm{am}) \le 1 \tag{a.21}$$

Gas Phase Methanol Synthesis. With the inherent difficulty of removing reaction heat, a strict constraint is imposed on the mole composition of inlet syngas to control the amount of reaction heat released for the gas phase methanol synthesis via setting an upper limit to the carbon to hydrogen ratio, as follows:

$$m_{\mathrm{b\_ms,t\_ms,s\vec{s}g,i}}(\mathrm{GP}, \mathrm{H_2}, t) - 2m_{\mathrm{b\_ms,t\_ms,s\vec{s}g,i}}(\mathrm{GP}, \mathrm{CO}, t) - 3m_{\mathrm{b\_ms,t\_ms,s\vec{s}g,i}}(\mathrm{GP}, \mathrm{CO_2}, t) \ge (y_{\mathrm{b\_ms}}(\mathrm{GP}) - 1)\cdot \mathrm{UB} \tag{a.22}$$

Mole flow rates of all components in the product gas and their mole compositions are expressed in terms of production rates of CH_3OH and H_2O, denoted as Δm_{meh} and Δm_{wat}, and stoichiometric coefficients of reaction r1 and r2, as follows:

$$\mathrm{CO} + 2\mathrm{H_2} \rightarrow \mathrm{CH_3OH} \tag{r1}$$

$$\mathrm{CO_2} + 3\mathrm{H_2} \rightarrow \mathrm{CH_3OH} + \mathrm{H_2O} \tag{r2}$$

$$m_{\mathrm{b\_ms,t\_ms,p\vec{g}m,o}}(\mathrm{am}, j, t) = m_{\mathrm{b\_ms,t\_ms,s\vec{s}g,i}}(\mathrm{am}, j, t) + v_1(j)\Delta m_{\mathrm{meh}} + v_2(j)\Delta m_{\mathrm{wat}}, \qquad j = \mathrm{is} \cap \mathrm{im} \tag{a.23}$$

Mole fractions of all components in the product gas are given by

$$\mathrm{ym}_{\mathrm{p\vec{g}m}}(\mathrm{am}, \mathrm{im}, t) = \frac{m_{\mathrm{b\_ms,t\_ms,p\vec{g}m,o}}(\mathrm{am}, \mathrm{im}, t)}{\sum_{\mathrm{im}} m_{\mathrm{b\_ms,t\_ms,p\vec{g}m,o}}(\mathrm{am}, \mathrm{im}, t)} \tag{a.24}$$

Fugacity coefficients of each component in the gaseous mixture are expressed in terms of mole fraction, critical temperature and pressure, and reaction temperature and pressure, as follows

$$\ln \phi(\mathrm{am}, \mathrm{im}, t) = \frac{9T_c(\mathrm{im})P}{128P_c(\mathrm{im})T}\left(1 - \left(\frac{T_c(\mathrm{im})}{\mathrm{T}}\right)^2\right)\mathrm{ym}_{\mathrm{p\vec{g}m}}(\mathrm{am}, \mathrm{im}, t) \tag{a.25}$$

The chemical equilibrium constants of reactions r1 and r2 are given below, in terms of mole fractions and fugacity coefficients of reactants.

$$K_1 = \frac{\mathrm{ym}_{\mathrm{p\vec{g}m}}(\mathrm{GP}, \mathrm{CH_3OH}, t)\phi(\mathrm{GP}, \mathrm{CH_3OH}, t)}{P^2\mathrm{ym}_{\mathrm{p\vec{g}m}}(\mathrm{GP}, \mathrm{CO}, t)\mathrm{ym}_{\mathrm{p\vec{g}m}}{}^2(\mathrm{GP}, \mathrm{H_2}, t)\phi(\mathrm{GP}, \mathrm{CO}, t)\phi^2(\mathrm{GP}, \mathrm{H_2}, t)} \tag{a.26}$$

$$K_2 = \frac{\mathrm{ym}_{\mathrm{p\vec{g}m}}(\mathrm{GP}, \mathrm{CO}, t)\mathrm{ym}_{\mathrm{p\vec{g}m}}(\mathrm{GP}, \mathrm{H_2O}, t)\phi(\mathrm{GP}, \mathrm{CO}, t)\phi(\mathrm{GP}, \mathrm{H_2O}, t)}{\mathrm{ym}_{\mathrm{p\vec{g}m}}(\mathrm{GP}, \mathrm{CO_2}, t)\mathrm{ym}_{\mathrm{p\vec{g}m}}(\mathrm{GP}, \mathrm{H_2}, t)\phi(\mathrm{GP}, \mathrm{CO_2}, t)\phi(\mathrm{GP}, \mathrm{H_2}, t)} \tag{a.27}$$

On the other hand, empirical equations of equilibrium constants K_1 and K_2 are given by the following expressions:

$$\log_{10} K_1 = \frac{3921}{T} - 7.971 \log_{10} T + 2.499 \times 10^{-3}T - 2.953 \times 10^{-7}T^2 + 10.2 \tag{a.28}$$

$$\ln K_2 = 4.33 - \frac{8240}{T + 460} \tag{a.29}$$

Thus relationships between component properties and reactor properties can be established through eqs a.26−a.29.

Liquid Phase Methanol Synthesis. For liquid phase methanol synthesis, equations of chemical equilibrium are set up for the liquid phase where catalytic reactions take place.

$$K_1 = \frac{x_{\mathrm{p\vec{g}m}}(\mathrm{CH_3OH}, t)k_{\mathrm{H}}(\mathrm{CH_3OH})\gamma(\mathrm{CH_3OH})}{x_{\mathrm{p\vec{g}m}}(\mathrm{CO}, t)x_{\mathrm{p\vec{g}m}}{}^2(\mathrm{H_2}, t)k_{\mathrm{H}}(\mathrm{CO})k_{\mathrm{H}}{}^2(\mathrm{H_2})\gamma(\mathrm{CO})\gamma^2(\mathrm{H_2})} \tag{a.30}$$

Henry's law constant k_{H} is given as follows.

$$k_{\mathrm{H}}(\mathrm{im}) = 10\mathrm{e}^{a(\mathrm{im})+(b(\mathrm{im})/T+c(\mathrm{im})\ln(T)}, \qquad \mathrm{im} = \mathrm{H_2}, \mathrm{CO}, \mathrm{CO_2}, \mathrm{N_2} \tag{a.31}$$

$$k_{\mathrm{H}}(\mathrm{im}) = 10^{(a'-b')/(T+c')}\cdot \phi(\mathrm{im}), \qquad \mathrm{im} = \mathrm{CH_3OH}, \mathrm{H_2O} \tag{a.32}$$

Activity coefficient γ for each reactant in the liquid phase, a solution comprising all reactants and inert oil, is obtained using the following expression.

$$\ln\gamma(\mathrm{im}, t) = 2A_{\mathrm{oil,im}}x_{\mathrm{p\vec{g}m}}(\mathrm{im}, t)x_{\mathrm{oil}}(\mathrm{oil}, t) + A_{\mathrm{im,oil}}x_{\mathrm{oil}}{}^2(\mathrm{oil}, t) - 2\sum_{\mathrm{im}} (A_{\mathrm{oil,im}}x_{\mathrm{p\vec{g}m}}{}^2(\mathrm{im}, t)x_{\mathrm{oil}}(\mathrm{oil}, t) + A_{\mathrm{im,oil}}x_{\mathrm{p\vec{g}m}}(\mathrm{im}, t)x_{\mathrm{oil}}{}^2(\mathrm{oil}, t)) \tag{a.33}$$

$$\sum_{\mathrm{im}} x_{\mathrm{p\vec{g}m}}(\mathrm{im}, t) + x_{\mathrm{oil}}(\mathrm{oil}, t) = 1 \tag{a.34}$$

where

$$A_{\mathrm{oil,im}} = a_{\mathrm{oil,im}} + b_{\mathrm{oil,im}}(T - 273.15) + c_{\mathrm{oil,im}}(T - 273.15)^2 \tag{a.35}$$

$$A_{\mathrm{im,oil}} = a_{\mathrm{im,oil}} + b_{\mathrm{im,oil}}(T - 273.15) + c_{\mathrm{im,oil}}(T - 273.15)^2 \tag{a.36}$$

With activity coefficients and fugacity coefficients available, phase equilibrium relationships between gaseous and liquid phases are established as

$$x_{\mathrm{p\vec{g}m}}(\mathrm{im}, t)\gamma(\mathrm{im}, t)k_{\mathrm{H}}(\mathrm{im}) = ym_{\mathrm{p\vec{g}m}}(\mathrm{LP}, \mathrm{im}, t)\phi(\mathrm{LP}, \mathrm{im}, t)P \quad (a.37)$$

The production rate of methanol is given by

$$m_{\mathrm{b\_ms,mep,o}}(t) = \sum_{\mathrm{am}} m_{\mathrm{b\_ms,t\_ms,p\vec{g}m,o}}(\mathrm{am}, \mathrm{im}, t), \quad \mathrm{im} = \mathrm{CH_3OH} \quad (a.38)$$

Moreover, it also should not exceed the capacity of the methanol synthesis block, as follows:

$$m_{\mathrm{b\_ms,mep,o}}(t) \le \mathrm{cap_{b\_ms}} \quad (a.39)$$

Production Rates. Production rates of primary products, i.e., methanol and electricity, and byproducts are calculated in this section.

Production of Methanol. The production rate of methanol is obtained from the methanol synthesis block, as follows:

$$\mathrm{ma_{meh}}(t) = \mathrm{MW(CH_3OH)} \cdot m_{\mathrm{b\_ms,meh,o}}(t) \quad (a.40)$$

The methanol production rate should not exceed its market demand in each period, given by

$$\mathrm{ma_{meh}}(t) \le \Phi_{\mathrm{meh}}(t) \quad (a.41)$$

Electricity Generation. Gross mechanical work is generated in the process from the gas and steam turbines. After deduction of the compression work consumed in the ASU, in the CO_2 capture block, and other auxiliary equipment, net mechanical work is obtained, as follows:

$$w_{\mathrm{net}}(t) = w_{\mathrm{grp}}(t) - w_{\mathrm{aia}}(t) - w_{\mathrm{aio}} - w_{\mathrm{ain}} - w_{\mathrm{b\_c1}}(t) - w_{\mathrm{b\_c2}} - w_{\mathrm{aux}}(t) - \Delta w^{\mathrm{wg}}(t) \quad (a.42)$$

Using the mechanical efficiency of the generator, the net electricity production rate is given by

$$\mathrm{elc}(t) = \eta_{\mathrm{m}} \cdot w_{\mathrm{net}}(t) \quad (a.43)$$

Again, the electricity production rate should not exceed its market demand in each period, as follows:

$$\mathrm{elc}(t) \le \Phi_{\mathrm{elc}}(t) \quad (a.44)$$

Production of Sulfur as a Byproduct. The production rate of sulfur is given as a product of sulfur removal rate and its content in the inlet coal, as follows:

$$\mathrm{ma_{sul}}(t) = \alpha_{\mathrm{sul/drc}}(\mathrm{ma}_{b\_\mathrm{cp,drc,i}}(t)\mathrm{UA(S)}) \quad (a.45)$$

Objective Functions. The NPV of the process is obtained by subtracting the total capital requirement up to the starting point of process operation from the summation of net profit in each period discounted to the same time point.

The calculation of the total capital requirement results from the investment cost calculations of primary equipment in all functional blocks. For each block, there is a reference capacity and investment cost. Size effects are considered by a size factor.

The investment cost of each block is given by

$$\mathrm{inv}(p, q) = \delta\mathrm{inv}(p, q)\left(\frac{\mathrm{cap}(p, q)}{\delta\mathrm{cap}(p, q)}\right)^{n}, \quad p = \mathrm{block}, q = \mathrm{technology} \quad (a.46)$$

After including investment costs for bulk plant items, engineering fees, project contingency, interest occurred during the construction period, and miscellaneous investment costs, the total investment cost can be obtained, denoted as $\mathrm{inv_{tcr}}$.

In each period, O and M costs includes purchase of feedstocks, sequestration of CO_2, and other fixed cost. Purchase of feedstocks is obtained as the product of capacity factor (availability), operating time within the period, price of feedstocks, and consumption rate, as follows

$$\mathrm{omc_{drc}}(t) = \lambda(t) \cdot \tau(t) \cdot \zeta_{\mathrm{drc}}(t) \cdot \mathrm{ma_{b\_cp,drc,i}}(t) \quad (a.47)$$

Income in each period comes from the sales of electricity and methanol (and sulfur as a byproduct), given by

$$\mathrm{inc_{elc}}(t) = \lambda(t) \cdot \tau(t) \cdot \zeta_{\mathrm{elc}}(t) \cdot \Phi_{\mathrm{elc}} \quad (a.48)$$

$$\mathrm{inc_{mep}}(t) = \lambda(t) \cdot \tau(t) \cdot \zeta_{\mathrm{mep}}(t) \cdot \Phi_{\mathrm{mep}} \quad (a.49)$$

$$\mathrm{inc_{sul}}(t) = \lambda(t) \cdot \tau(t) \cdot \zeta_{\mathrm{sul}}(t) \cdot \mathrm{ma_{sul}}(t) \quad (a.50)$$

The net income in each period is thus obtained as follows

$$\mathrm{inc_{net}}(t) = (\mathrm{inc_{elc}}(t) + \mathrm{inc_{mep}}(t) + \mathrm{inc_{sul}}(t)) - (\mathrm{omc_{drc}}(t) + \mathrm{omc_{seq}}(t) + \mathrm{omc_{fix}}(t)) \quad (a.51)$$

After discounting the net income in all periods to the starting point of project, the net present value is obtained as follows

$$\mathrm{npv} = \sum_{t} \frac{\mathrm{inc_{net}}}{(1 + r)^{\tau(t)}} - \mathrm{inv_{tcr}} \quad (a.52)$$

Equation a.52 is used as the objective function to be maximized.

Model Summary. The entire model is a nonconvex MINLP problem, summarized as follows:

$$\begin{aligned} &\max \quad f = \mathrm{npv} \\ &\mathrm{s.t.} \quad \mathrm{eq\ a.1{-}a.52} \\ &\text{mass and energy balances for all other functional blocks} \end{aligned} \quad (a.53)$$

Appendix B: Illustration of the Cubature Based Integration Technique

Assume there are five uncertain parameters, namely the coal price, the electricity price, the methanol price, the electricity demand, and the methanol price, i.e., $N_\theta = 5$, the formula with the smallest N_{p} is the specialized cubature of degree five of type one, denoted as $SC_{5,1}$. The relation between N_{p} and N_θ is given as follows:

$$N_{\mathrm{p}} = 2^{N_\theta} + 2N_\theta = 42 \quad (b.1)$$

The means of generation of normalized sampling points u_i and corresponding weights B_i is given as follows:

$$\begin{matrix} (r, 0, ..., 0)B_0 \\ (s, s, ..., s)B_1 \end{matrix} \quad (b.2)$$

where the length of both vectors is N_θ. Formulations of r, s, B_0, and B_1 are given as follows:

$$r^2 = \frac{N_\theta + 2}{4} \quad (b.3)$$

$$s^2 = \frac{N_\theta + 2}{2(N_\theta - 2)} \tag{b.4}$$

$$B_0 = \frac{4}{(N_\theta + 2)^2}V \tag{b.5}$$

$$B_1 = \frac{(N_\theta - 2)^2}{2^{N_\theta}(N_\theta + 2)^2}V \tag{b.6}$$

$$V = \pi^{N_\theta/2} \tag{b.7}$$

Notation

Sets

ac = syngas cleanup technologies
ag = gasification technologies
agt = gas turbine technologies
am = methanol synthesis technologies, GP for gas phase, LP for liquid phase
ia = components in the air: O_2, N_2
im = components in product gas of methanol synthesis: N_2, H_2O, H_2, CO, CO_2, CH_3OH
is = components in syngas: H_2, CO, CO_2, H_2O, N_2, H_2S
t = time interval

Parameters

Φ = market demand for each primary product, MW for electricity, tonne/day for methanol
$\alpha_{bld/drc}$ = mass ratio between blown down water and inlet coal for a gasifier
$\alpha_{csl/drc}$ = mass ratio between water and coal in coal slurry
$\alpha_{hyd/cm}$ = mass ratio between H_2 and CO in crude syngas
$\alpha_{mkw/drc}$ = mass ratio between making-up water and inlet coal for a gasifier
$\alpha_{oxb/drc}$ = mass ratio between oxygen and coal in oxygen-blown pulverized coal feed
$\alpha_{oxy/drc}$ = mass ratio between inlet oxygen and coal steams to a gasifier
α_{rch/b_gs} = heat recovery rate in the gasifier chamber and scrubber block
$\alpha_{ssl/drc}$ = mass ratio between slag slurry from the syngas scrubber and inlet coal to a gasifier
$\alpha_{sul/drc}$ = recovery rate of sulfur
$\alpha_{swi/drc}$ = mass ratio between steam/water injection and inlet coal for a gasifier
η_i = internal efficiency
η_m = mechanical efficiency
λ = capacity factor (availability)
τ = operating time, hour
υ = stoichiometric coefficient
ζ = price, \$/(kW h) for electricity, \$/metric tonne for others
A = coefficient for calculation of activity coefficient of a component solved in inert oil
K = equilibrium constant
MW = molecular weight
P = pressure, bar
P_c = critical pressure, bar
T = temperature, K
T_c = critical temperature, K
UA = ultimate analysis of coal, comprising C, H, O, N, S, ash, wt %
UB = upper bound
X_{air} = mole composition of air
X_{ani} = mole composition of nitrogen stream produced in ASU
X_{aox} = mole composition of oxygen stream produced in ASU
a = coefficient for calculation of Henry's law constant
a' = coefficient for calculation of Henry's law constant
$a_{im,oil}$ = coefficient for calculation of activity coefficient
$a_{oil,im}$ = coefficient for calculation of activity coefficient
b = coefficient for calculation of Henry's law constant
b' = coefficient for calculation of Henry's law constant
$b_{im,oil}$ = coefficient for calculation of activity coefficient
$b_{oil,im}$ = coefficient for calculation of activity coefficient
c = coefficient for calculation of Henry's law constant
c' = coefficient for calculation of Henry's law constant
$c_{im,oil}$ = coefficient for calculation of activity coefficient
$c_{oil,im}$ = coefficient for calculation of activity coefficient
h = enthalpy, kJ/mol
k_H = Henry's law constant
n = size factor
r = discount rate
r_{inf} = inflation rate
x^* = steam quality

Binary Variables

y = selection of equipment using a technology, 1 for selection, 0 otherwise

Continuous Variables

Δm_{meh} = production rate of methanol in methanol synthesis block, kmol/s
Δm_{wat} = production rate of water in methanol synthesis block, kmol/s
ϕ = fugacity coefficient
cap = capacity of a functional block
elc = electricity generation, MW
h = enthalpy flow rate, MJ/s (MW)
inc = income, million dollar
inv = investment cost for equipment, million dollar
m = mole flow rate, kmol/s
ma = mass flow rate, kg/s
npv = net present value, million dollar
omc = O and M cost, million dollar
w = mechanical work, MW
x = mole fraction for liquid phase
ym = mole fraction for gaseous phase
z = streams upon which capacity of a block is defined

Subscripts

Functional Blocks

b_as = air separation unit
b_cp = coal preparation
b_ms = methanol synthesis
b_gs = gasifier chamber and scrubber

Technologies

t_gs = gasification technologies
t_ms = methanol synthesis technologies, GP for gas phase, LP for liquid phase

Components

air = overall air flow
aia = atmosphere air
aic = compressed air
bld = blown down water
csg = crude syngas
csl = coal slurry
drc = dry coal

elc = electricity
mep = methanol product
mkw = making up water
nit = nitrogen
oil = inert oil in liquid phase methanol synthesis
oxy = oxygen
pgm = product gas from methanol synthesis block
ssl = slag slurry
sul = element sulfur
swi = steam/water injection

Positions

i = inlet
o = outlet

Miscellaneous

fix = fixed O and M cost
ist = interest
net = net production rate/income
tpc = total plant cost

Literature Cited

(1) Larson, E. D.; Wu, Z. X.; DeLaquil, P.; Chen, W. Y.; Gao, P. F. Future implications of China's energy-technology choices. *Energy Policy* **2003**, *31*, 1189–1204.

(2) Li, Z.; Ni, W. D.; Zheng, H. T.; Ma, L. W. Polygeneration energy system based on coal gasifi- cation. *Energy Sustainable Dev.* **2003**, *7*, 57–62.

(3) Gao, L.; Jin, H.; Liu, Z.; Zheng, D. Exergy analysis of coal-based polygeneration system for power and chemical production. *Energy* **2004**, *29*, 2359–2371.

(4) Hetland, J.; Li, Z.; Xu, S. S. How polygeneration schemes may develop under an advanced clean fossil fuel strategy under a joint sino-European initiative. *Appl. Energy* **2009**, *86*, 219–229.

(5) Serra, L. M.; Lozano, M.-A.; Ramos, J.; Ensinas, A. V.; Nebra, S. A. Polygeneration and efficient use of natural resources. *Energy* **2009**, *34*, 575–586.

(6) Qian, Y.; Liu, J. Y.; Huang, Z. X.; Kraslawski, A.; Cui, J.; Huang, Y. L. Conceptual design and system analysis of a poly-generation system for power and olefin production from natural gas. *Appl. Energy* **2009**, *86*, 2088–2095.

(7) *U.S., Clean Coal Technology Programs: Program Update 2003 (Volume 1)*; Technical Report DOE/FE-0459-1, Department of Energy: Washington, D.C., 2003.

(8) Liu, P.; Gerogiorgis, D. I.; Pistikopoulos, E. N. Modeling and optimization of polygeneration energy systems. *Catal. Today* **2007**, *127*, 347–359.

(9) Liu, P.; Pistikopoulos, E. N.; Li, Z. A mixed-integer optimization approach for polygeneration energy systems design. *Comput. Chem. Eng.* **2009**, *33*, 759–768.

(10) Liu, P.; Pistikopoulos, E. N.; Li, Z. A multi-objective optimization approach to polygeneration energy systems design. *AIChE J.*, published online Oct 1, 2009, http://dx.doi.org/10.1002/aic.12058.

(11) Pistikopoulos, E. N. Uncertainty in process design and operations. *Comput. Chem. Eng.* **1995**, *19*, 553–563.

(12) Ierapetritou, M. G.; Pistikopoulos, E. N. Novel Optimization Approach of Stochastic Planning Models. *Ind. Eng. Chem. Res.* **1994**, *33*, 1930–1942.

(13) Ahmed, S.; Sahinidis, N. V.; Pistikopoulos, E. N. An improved decomposition algorithm for optimization under uncertainty. *Comput. Chem. Eng.* **2000**, *23*, 1589–1604.

(14) Liu, P.; Pistikopoulos, E. N.; Li, Z. Global multi-objective optimization of a nonconvex MINLP problem and its application on polygeneration energy systems design, CMU-IBM Cyber- Infrastructure for MINLP. http://www.minlp.org/library/index.php (accessed Dec 2009).

(15) *GAMS - A user's guide*; GAMS Development Corporation; http://www.gams.com/docs/gams/GAMSUsersGuide.pdf (accessed Dec 2009).

(16) Sahinidis, N.; Tawarmalani, M. *BARON*; GAMS Development Corporation; http://www.gams.com/solvers/solvers.htm (accessed Dec 2009).

(17) Birge, J. R.; Louveaux, F. V. *Introduction to stochastic programming*; Springer: New York, 1997.

(18) Kall, P.; Wallace, S. W. *Stochastic programming*; John Wiley & Sons: Chichester, 1994.

(19) Sahinidis, N. V. Optimization under uncertainty: state-of-the-art and opportunities. *Comput. Chem. Eng.* **2004**, *28*, 971–983.

(20) Stroud, A. H. *Approximate calculation of multiple integrals*; Prentice Hall: London, 1971.

(21) Engels, H. *Numerical quadrature and cubature*; Academic Press: London, 1980.

(22) Bernardo, F. P.; Pistikopoulos, E. N.; Saraiva, P. M. Integration and computational issues in stochastic design and planning optimization problems. *Ind. Eng. Chem. Res.* **1999**, *38*, 3056–3068.

(23) Floudas, C. A.; Aggarwal, A.; Ciric, A. R. Global optimum search for nonconvex NLP and MINLP problems. *Comput. Chem. Eng.* **1989**, *13*, 1117–1132.

(24) Ryoo, H. S.; Sahinidis, N. V. Global optimization of nonconvex NLPs and MINLPs with applications in process design. *Comput. Chem. Eng.* **1995**, *19*, 551–566.

(25) Lee, S. *Methanol Synthesis Technology*; CRC Press: Boca Raton, FL, 1990.

Received for review September 23, 2009
Revised manuscript received January 8, 2010
Accepted February 4, 2010

IE901490G